2024 IEEE/RSJ International Conference on Intelligent Robots and Systems (IROS)
October 14-18, 2024. Abu Dhabi, UAE

Dynamics-Based Trajectory Planning for Vibration Suppression of a Flexible Long-Reach Robotic Manipulator System*

Anthony Siming Chen[1], Erwin Jose Lopez Pulgarin[1], Guido Herrmann[1], Alexander Lanzon[1], Joaquin Carrasco[1], Barry Lennox[1], Benji Carrera-Knowles[2], John Brotherhood[2], Tomoki Sakaue[3], and Kaiqiang Zhang[4]

***Abstract*— We address the unique challenge of vibration suppression for a flexible long-reach robotic manipulator system, namely, the through-wall deployment (TWD) system that is used in nuclear environments. This paper proposes a novel dynamics-based trajectory optimization approach, which minimizes both the acceleration and the jerk at the manipulator's joints, as well as the vibrations of the flexible long-reach boom where the manipulator's base is mounted. Firstly, we create an integrated model for the system dynamics based on the knowledge of the robotic manipulator and the acceleration data from the vibration tests. We then develop an original procedure for generating the high-order polynomial trajectory that guarantees the zero-boundary condition for a flexible number of optimization parameters and waypoints. Following the simulation of a multi-objective optimization scheme, the optimized trajectory is experimentally validated on the practical TWD system with around 28% vibration reduction on average compared to the benchmark. Importantly, this reduction is achieved without compromising on the average speed of motion. The methodology is transferable to a wider range of flexible robotic manipulator systems with similar characteristics.**

***Index Terms*— Flexible robotics, trajectory planning, optimization, vibration suppression, nuclear robotics**

I. INTRODUCTION

The use of robots for remote maintenance often requires installing a robot in unconventional flexible structures. This research is directly motivated by the pressing need for vibration control of the *through-wall deployment* (TWD) system used in nuclear decommissioning, which comprises a rigid robotic manipulator mounted at the end of a flexible long-reach two-link boom. The aim of this study is to develop a trajectory planning approach that can compensate for the modal flexibility of the long-reach boom through the appropriate actuation of the robotic manipulator. From the control's perspective, trajectory planning can be viewed as an open-loop or feedforward control approach. This is extremely useful in our case, i.e., a challenging radioactive nuclear environment, as it eliminates the demand for extra sensors or actuators. Most existing trajectory planning methods for robotic manipulators consider grasping/handling objects or avoiding obstacles, where the base of a manipulator is usually assumed to be fixed at a rigid base. The trajectories within either the joint space or the task space are designed concerning general features such as initial/final point, duration, maximum velocity, etc., while the vibration it generates to the environment or the vibration of the manipulator itself is often neglected.

A. Related Work

Optimization is the core of trajectory or path planning. A trajectory is usually optimized based on its energy efficiency, execution time, actuator torque, or a combination of them. Some comprehensive surveys can be found in [1]–[4]. However, the optimality criteria do not often include vibration. There is generally a lack of understanding of how the motion of a manipulator's joints and end effector excites vibration at its base, not to mention when the base is flexible. It should be distinguished that our flexible long-reach robotic manipulator system is a combination of a rigid industrial manipulator and a flexible long-reach boom, which is different from common flexible manipulators [5]–[10] where the manipulator itself (one or more links) is flexible. Therefore, most of the vibration control methods for flexible manipulators, such as [5]–[10], cannot be applied here directly. Among the above literature, it is found that the work in [10] proposed a trajectory optimization method via particle swarm for suppressing residual vibrations in a two-link "rigid-flexible" manipulator, where the first link is rigid, and the second link is flexible. This structure might appear similar to our system. However, our system requires the actuation of the "rigid" link (the 6-joint manipulator) to suppress the vibration of its base, the "flexible" link (the boom), whereas in [10], the trajectory optimization was carried out for a single joint (the second joint) and the first joint was assumed to follow a cycloidal motion. More recently, a trajectory optimization approach, also employing particle swarm, was provided in [11], where their system is essentially the same structure as our system (whilst their rigid

*The work was funded by the UK Atomic Energy Authority (UKAEA) within the scope of the LongOps program. The work was partially funded by the Advanced Machinery Productivity Institute (AMPI), and supported by UKAEA/EPSRC Fusion Grant 2022/27 (EP/W006839/1) for fusion decommissioning.

[1]A.S. Chen, E.J. Lopez Pulgarin, G. Herrmann, A. Lanzon, J. Carrascro, and B. Lennox are with the Control Systems and Robotics (CSR) Group, Department of Electrical and Electronic Engineering, The University of Manchester, M13 9PL Manchester, United Kingdom. Email for A.S. Chen: siming.chen@manchester.ac.uk

[2]B. Carrera-Knowles and J. Brotherhood are with Jacobs, 601 Faraday Street, Birchwood, Warrington, WA3 6GN, United Kingdom. Email for J. Brotherhood: john.brotherhood@jacobs.com

[3]T. Sakaue is with Tokyo Electric Power Company (TEPCO) Holdings, Fukushima, Japan. sakaue.tomoki@tepco.co.jp

[4]K. Zhang is with the United Kingdom Atomic Energy Authority (UKAEA), Culham Campus, OX14 3DB, United Kingdom. kaiqiang.zhang@ukaea.uk

manipulator was assumed to be made of 3 identical links for simplicity). Although without experimental validation, their numerical simulation demonstrates the effectiveness of minimizing the vibration at the end of the flexible beam by optimizing the parameters of a polynomial trajectory.

B. Contributions

In this paper, we address the unique challenge of vibration suppression for the TWD system in nuclear environments by developing a new dynamics-based trajectory planning approach. Rather than planning for a low-bandwidth control and slow path of the robotic manipulator, the focus will be on a clear understanding of the dynamic interaction of the manipulator and the boom which allows controlling the robotic manipulator in such a way to avoid the excitation of the boom and achieve fast control of the manipulator. In that way, the robotic manipulator will employ significant elements of feedforward approaches, which can be employed also in an optimization framework. The novelty of this work lies in the combination of dealing with a flexible dual-link long boom robotic system in the context of sensor-limited information, which requires a strong combination of optimal feedforward and path planning to avoid excitation of the modal resonances of the flexible long boom system when the multi-degree-of-freedom manipulator is in fast motion. This work provides the following contributions:

1) A novel dynamics-based trajectory optimization scheme is proposed considering both the acceleration and the jerk at joints, as well as the knowledge of the system (modified transfer functions for the dominant modes).

2) An original procedure is developed for generating the high-order polynomial trajectory that guarantees the zero boundary condition for a *flexible* number of optimization parameters and a *flexible* number of waypoints.

3) The optimized trajectory is experimentally validated on the practical TWD system. The methodology is transferable to a wider range of flexible long-reach robotic manipulator systems with similar characteristics.

The rest of the paper is structured as follows. Section II introduces the TWD system model. Section III presents the new trajectory design and its multi-objective optimization scheme. Section IV provides the simulations and experimental validation of the proposed dynamics-based trajectory planning method. Section V concludes the paper with discussions and possible future research directions.

II. TWD SYSTEM MODEL

The TWD system consists of two parts: 1) a flexible long-reach boom and 2) a rigid robotic manipulator. Assuming the manipulator is a rigid body, the vibration of the end effector is directly translated from the vibration at the end of the boom since the manipulator base is mounted there. Therefore, we focus on understanding the modal characteristics of the boom, i.e., how the force or torque generated from the manipulator translates to the vibration of the boom's end. This also provides a better understanding of the robotic manipulator in relation to its environment.

A set of vibration tests were carried out covering a wide range of the operating conditions of the flexible long-reach boom, which includes 4 configurations while the robotic manipulator remains fixed and non-actuated (see Fig. 1).

Fig. 1: Photographs of the 4 boom configurations (Configuration 1: Full-length boom with 180-degree hinge angle; Configuration 2: Full-length boom with 90-degree hinge angle; Configuration 3: Full-length boom with 45-degree hinge angle; Configuration 4: Half-length boom with 180-degree hinge angle).

These vibration data provide a set of *frequency response functions* (FRFs), which formed the basis for a control-focused TWD dynamical model, i.e., a nonlinear dynamic model of the robotic manipulator and a robust, yet simple, model for the boom modal characteristics. The model is created in MATLAB/Simscape. It can be adjusted to reflect the 4 different configurations of the boom by loading the transfer function parameters that correspond to the FRFs.

III. MULTI-OBJECTIVE TRAJECTORY OPTIMIZATION

This section proposes the trajectory planning for the robotic manipulator of the TWD system. It has been observed that the vibration at the end of the boom is caused by the motion of the robotic manipulator, where relatively higher vibration magnitude occurs when the motion has high or non-smooth acceleration, e.g., when the non-optimized trajectory starts and stops. The key factors contributing to the vibration can be explained by a non-smooth starting or stopping motion where the acceleration or the variation of acceleration, i.e., the jerk, is high at the starting/stopping time instance or over the whole joint motion period.

A. High-Order Polynomial Trajectory Generation: A Novel Zero-Boundary Approach

We propose a new high-order polynomial trajectory to guarantee the zero-boundary condition for a flexible number of optimization parameters. It should be distinguished from the standard minimum acceleration/jerk trajectories with a fixed number of parameters [12]–[14] derived via the Euler-Lagrangian method.

We first write down the n^{th} order polynomial trajectory in terms of its position, velocity, acceleration, and jerk with respect to time $t \geq 0$ for $n \in \mathbb{N}^+$:

$$\text{Position } x(t) = c_0 + c_1 t + c_2 t^2 + \cdots + c_{n-1} t^{n-1} + c_n t^n, \tag{1}$$

$$\text{Velocity } \dot{x}(t) = c_1 + 2c_2 t + 3c_3 t^2 + \cdots + (n-1)c_{n-1} t^{n-2} + n c_n t^{n-1}, \tag{2}$$

$$\text{Acceleration } \ddot{x}(t) = 2c_2 + 6c_3 t + 12c_4 t^2 + \cdots + (n-1)(n-2)c_{n-1} t^{n-3} + n(n-1)c_n t^{n-2}, \tag{3}$$

$$\text{Jerk } \dddot{x}(t) = 6c_3 + 24c_4 t + 60c_5 t^2 + \cdots + (n-1)(n-2)(n-3)c_{n-1} t^{n-4} + n(n-1)(n-2)c_n t^{n-3}, \tag{4}$$

where $c_0, c_1, c_2, \cdots, c_n$ are the design parameters for the polynomial trajectory.

Motivated by the fact that more vibration occurs when starting and stopping a motion, we can apply m constraints to the boundary conditions of a polynomial trajectory with $m \in \mathbb{N}^+$. Considering the 8 constraints for zero velocity, acceleration, and jerk at the starting point $x(0) = a$ at the time $t = 0$ and end point $x(T) = b$ at the time $t = T$ $(T > 0)$, i.e., $m = 8$, we have

$$x(0) = a, \quad \text{(5a)} \qquad x(T) = b, \quad \text{(5e)}$$
$$\dot{x}(0) = 0, \quad \text{(5b)} \qquad \dot{x}(T) = 0, \quad \text{(5f)}$$
$$\ddot{x}(0) = 0, \quad \text{(5c)} \qquad \ddot{x}(T) = 0, \quad \text{(5g)}$$
$$\dddot{x}(0) = 0, \quad \text{(5d)} \qquad \dddot{x}(T) = 0. \quad \text{(5h)}$$

We refer to these constraints as the zero-boundary condition in this paper. Then we can rewrite the above m constraints using (1)-(4) into (7) or a more compact form:

$$PC = L, \tag{6}$$

where $n \geq m \in \mathbb{N}^+$; P is the m by $n+1$ coefficient matrix; C and L are the $(n+1)$-dimensional parameter and m-dimensional boundary condition vectors, respectively, as shown in (7) in the next page. When $n = m$, the trajectory is uniquely determined by the eight constraints. But when $n > m$, we will have $n - m$ free coefficients to be optimized while the $m = 8$ boundary conditions are guaranteed. Thus, we can design a polynomial trajectory with order higher than 8. The higher the order, the more free design parameters can be used for optimization. Moreover, one can add multiple waypoints to the polynomial trajectory. Any additional waypoint is considered to be a boundary condition, which will be introduced to the optimization problem. Similarly, additional configurations, e.g., velocity or acceleration, of a waypoint can be introduced as additional boundary conditions of the optimization problem.

We now formulate our original procedure for generating the polynomial trajectory with the zero-boundary condition. The high-order polynomial position trajectory (1) can now be written simply as

$$x(t) = \begin{bmatrix} 1 & t & t^2 & \cdots & t^n \end{bmatrix} C. \tag{8}$$

with the parameter vector C to be determined. Applying *singular value decomposition* (SVD) for the zero-boundary condition (5) or (7) (in the following page), we have

$$U \begin{bmatrix} \Sigma_r & 0 \end{bmatrix} V^{\mathsf{T}} C = L, \tag{9}$$

where U is a unitary matrix, Σ_r is a diagonal matrix with non-negative real numbers on the diagonal, $V = \begin{bmatrix} V_r & V_0 \end{bmatrix}$ is a complex unitary matrix, i.e., V_r corresponding to Σ_r. Therefore, we can express the part of the parameter vector C that can be determined by the zero-boundary condition as

$$C_{\text{fixed}} = \Sigma_r^{-1} U^{\mathsf{T}} L, \tag{10}$$

with C_{fixed} being the 8-dimensional vector with fixed parameters and the following relation

$$C = \begin{bmatrix} V_r & V_0 \end{bmatrix} \begin{bmatrix} C_{\text{fixed}} \\ C_{\text{free}} \end{bmatrix}, \tag{11}$$

where V_r and V_0 are extracted from V; C_{free} denotes the free design parameters to be determined via optimization.

Therefore, the high-order polynomial trajectory (8) can now be determined by

$$x(t) = \begin{bmatrix} 1 & t & t^2 & \cdots & t^n \end{bmatrix} \begin{bmatrix} V_r & V_0 \end{bmatrix} \begin{bmatrix} \Sigma_r^{-1} U^{\mathsf{T}} L \\ C_{\text{free}} \end{bmatrix}, \tag{12}$$

with C_{free} being the only unknown in the above equation, i.e., the design parameters.

B. Multi-Objective Optimization

The proposed zero-boundary approach for generating high-order polynomial trajectory offers the flexibility to optimize the trajectory in terms of a prescribed cost function. One can write a conventional cost function, e.g. in [13], [14], for minimizing many temporal derivatives of the trajectory at the same time:

$$J(x) = \int_0^T [w_0 x(t)^2 + w_1 \dot{x}(t)^2 + \cdots + w_n (\frac{d^n x(t)}{dt^n})^2] dt, \tag{13}$$

where $w_0, w_1, \cdots, w_n$ are non-negative weight constants. optimizing such cost function allows a sufficiently smooth trajectory:

$$x^*(t) = \arg\min_{x(t)} J(x). \tag{14}$$

In this paper, by leveraging the knowledge of the system dynamics (the model) and focusing only the the second and third derivatives, i.e., acceleration and jerk, we decide to augment this cost function (13) within a multi-objective optimization framework:

$$J'(x) = \int_0^T [w_0 \ddot{x}(t)^2 + w_1 \dddot{x}(t)^2 + w_3 \hat{a}_x^2 + w_4 \hat{a}_y^2] dt, \tag{15}$$

where $\hat{a}_x$ and $\hat{a}_y$ are the vertical and horizontal outputs from the boom model, which denote the nominal acceleration on X and Y axis directions. minimizing the new cost function (15) over the trajectory (12) results in minimizing the acceleration, the jerk, and the vibration (acceleration) at the end of the boom (available from transfer function outputs in the simulation model). Thus, the parameters C_{free} in (12) are optimized based on the system dynamics.

$$\begin{bmatrix} 1 & 0 & 0 & 0 & \cdots & 0 & 0 \\ 0 & 1 & 0 & 0 & \cdots & 0 & 0 \\ 0 & 0 & 2 & 0 & \cdots & 0 & 0 \\ 0 & 0 & 0 & 6 & \cdots & 0 & 0 \\ 1 & T & T^2 & T^3 & \cdots & T^{n-1} & T^n \\ 0 & 1 & 2T & 3T^2 & \cdots & (n-1)T^{n-2} & nT^{n-1} \\ 0 & 0 & 2 & 6T & \cdots & (n-1)(n-2)T^{n-3} & n(n-1)T^{n-2} \\ 0 & 0 & 0 & 6 & \cdots & (n-1)(n-2)(n-3)T^{n-4} & n(n-1)(n-2)T^{n-3} \end{bmatrix} \begin{bmatrix} c_0 \\ c_1 \\ c_2 \\ c_3 \\ \vdots \\ c_{n-1} \\ c_n \end{bmatrix} = \begin{bmatrix} a \\ 0 \\ 0 \\ 0 \\ b \\ 0 \\ 0 \\ 0 \end{bmatrix} \tag{7}$$

IV. SIMULATION AND EXPERIMENTAL VALIDATION

We study a common case in nuclear decommissioning in which the robotic manipulator is required to move to a set of points at specific time instances. The case study includes simulation and experimental validation.

A. Simulation

Here we start by explaining the simulation in terms of a single-position trajectory in the joint space. For example, Joint 2 is required to move based on the 5 positions sequentially: 1) 0° at $t = 0$ s, 2) 10° at $t = 3$ s, 3) 60° at $t = 6$ s, 4) 30° at $t = 9$ s, and 5) 50° at $t = 12$ s. To complete this task, one can simply control the robotic manipulator by setting up the target points sequentially via the teach pendant. By default setting, this will return a set of motions of Joint 2 with a constant speed. We refer to this method as a benchmark. Alternatively, using the proposed approach in this paper, we can generate a 12^{th}-order polynomial trajectory for the Joint 2 position using (12) because the task is equivalent to moving from one point to another via 3 waypoints[1]. Therefore, the number of parameters is 13 including 8 fixed parameters due to the zero-boundary condition, 3 fixed parameters due to the waypoints' position, and 2 free parameters to be optimized (here $n = 12$ and $m = 8 + 3 = 11$). The cost function is selected as (15) with the weights w_0, w_1, w_3, and w_4 being properly adjusted.

As discussed earlier, the model is created by integrating the robotic manipulator model with the boom model. Given that the system dynamics are inherently highly nonlinear, we use the *sequential quadratic programming* (SDP) algorithm, i.e., a quasi-Newton method in constrained nonlinear optimization, with a gradient descent method for optimizing the 2 free parameters of the 12^{th}-order polynomial trajectory. In practice, there are many factors contributing to how long it takes to compute a specific trajectory. This depends on the optimization method, the algorithm, the parameter tolerance, the maximum iterations, etc. Empirically, running an optimization with only acceleration and jerk in the cost function usually takes only a few minutes while, in this paper, running an optimization that also considers the system dynamics via the simulation model will take even longer computational time. As a result, the values of the 13 parameters for Joint 2 after optimization are $[1.666 \times 10^{-12},\ 2.865 \times 10^{-10},\ 3.568 \times 10^{-8},\ 2.651 \times 10^{-6},\ 3.371 \times 10^{-4},\ 9.209 \times 10^{-3},\ 0.04906,\ -8.951 \times 10^{-3},\ 3.648 \times 10^{-3},\ 1.796 \times 10^{-4},\ 1.42 \times 10^{-3},\ -1.598,\ 0.2141]^{\mathsf{T}}$, where the first 11 parameters are the fixed parameters and the last 2 parameters are the optimized free parameters. We will show the benchmark and optimized trajectories later in the experimental validation. Now we may check some preliminary vibration results of the two trajectories via the simulation model. To assess their overall performance of vibrations, we define the following integral squared vibration metric ($h = 30$ s):

$$\mu = \frac{1}{2}\left(\int_0^h \hat{a}_x^2(t)dt + \int_0^h \hat{a}_y^2(t)dt\right). \tag{16}$$

Here, we start the trajectories for Joint 2 when the manipulator is stationary, i.e. no initial vibration, then we continue the measurement of the nominal accelerations on X and Y axis directions after the trajectories are finished until $t = 30$s to take into account the residual vibration. Table I shows the comparison of the two trajectories in simulations.

TABLE I: Preliminary results: vibration comparison of the two trajectories in simulations.

	Benchmark trajectory	Optimized trajectory
Vibration metric μ	2.6×10^{-5}	8.45×10^{-6}
Vibration reduction	-	67.5%

B. Experimental Validation

Now we show the validation of the proposed trajectory planning approach through practical experiments on the TWD system.

The benchmark and the optimized trajectories are tested in the above-mentioned experimental setup. We created the optimized trajectories on MATLAB and exported them as a CSV file, which contained the expected joint position per time step. We connected to the M1013 Doosan control box using an Ethernet Gigabit connection at 100 Hz. We used their programming API, Doosan Robotics Framework Library (DRFL), and the ROS1 framework to control and interact with the robot. We used ROS1 for data logging of the joint states at 100 Hz. The function "*movej*" was used to send the whole trajectory at a time. Each trajectory consisted

[1]A waypoint refers to a specific point or position that the trajectory should pass through. Here it is possible to choose any higher-order polynomial above 12^{th}-order for a trajectory with 3 waypoints. The higher order, the more free parameters are available for optimization. Choosing a 12^{th}-order polynomial implies the trade-off between the computational cost and performance.

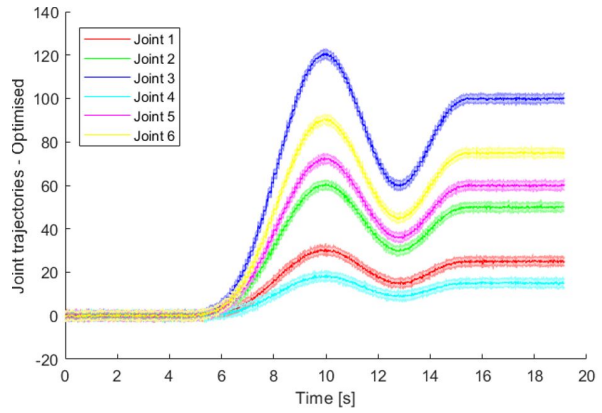

Fig. 2: Joint positions measurement [°] – optimized based on the acceleration, jerk, and system dynamics.

of 100 points at a time, discretized at 10 Hz; these numbers were found experimentally as the largest number of points the robot could process at a time and the ideal time per step.

In the experiments, the trajectory optimization procedure in the above simulation is applied to all six joints of the robotic manipulator with different target positions. Fig. 2 depicts the measurement of the six joints' positions. It is obvious that the optimized trajectories pass each target point smoothly. We present the acceleration measurement (vertical and horizontal) of all 4 boom configurations in Fig. 3. By comparing each subplot in Fig. 3a (benchmark) and in Fig. 3b (optimized), it is noted that the absolute peak values of accelerations are sometimes not reduced, e.g., the vertical acceleration comparison of Configuration 3, however, the residual vibrations are significantly suppressed for all the cases. To capture the overall behaviour of the accelerations, we also calculate the peak vibration reduction, i.e., the maximum acceleration minus the minimum acceleration, as well as the vibration metric μ (16) for the vibration evaluation. Each experimental trajectory was repeated for 3 times to obtain the average vibration reduction with the deviation. Table II demonstrates the vibration reduction results for all 4 configurations. It is obvious that the vibration is suppressed significantly in terms of reducing the peak as well as the overall magnitude. On average, the proposed dynamics-based optimization approach results in 28.74% peak reduction and 28.38% overall reduction. Notably, this reduction is achieved without compromising on the average speed of motion.

TABLE II: Experimental results: vibration reduction of the optimized trajectories against the benchmark trajectories.

Boom configuration	Vibration reduction (peak)	Vibration reduction (overall)
Configuraton 1	$29.95\% \pm 5\%$	$23.68\% \pm 3\%$
Configuraton 2	$49.24\% \pm 4\%$	$52.15\% \pm 4\%$
Configuraton 3	$7.07\% \pm 1\%$	$22.74\% \pm 2\%$
Configuraton 4	$28.68\% \pm 4\%$	$14.94\% \pm 1\%$
Average	28.74%	28.38%

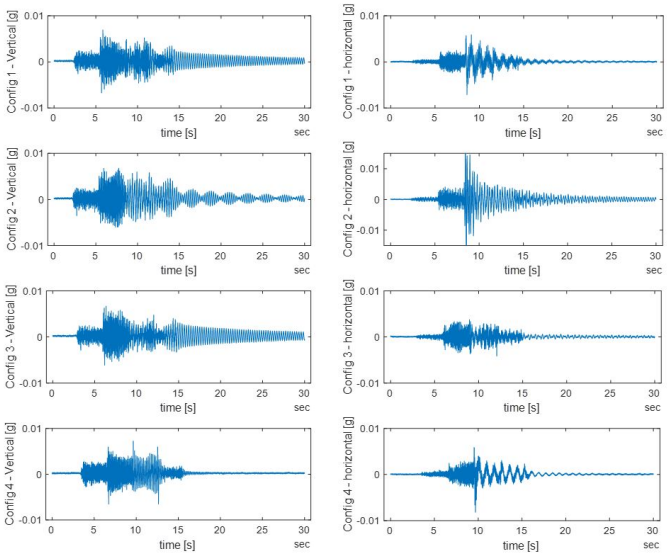

(a) Vertical (left column) and horizontal (right column) accelerations under the 4 Configurations - Benchmark joint trajectories.

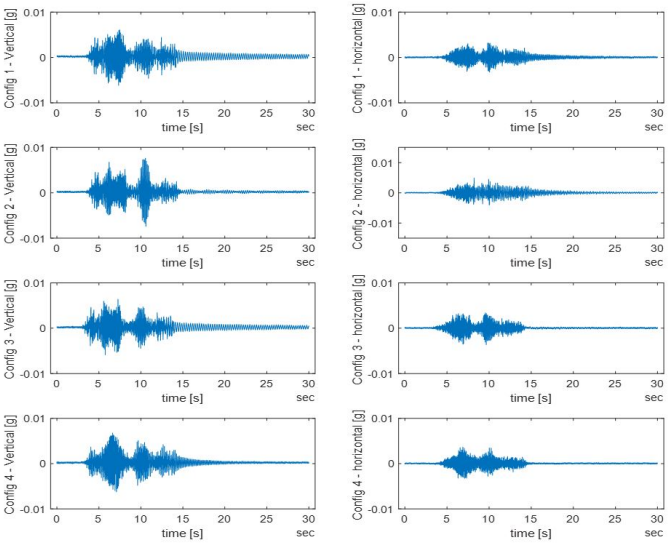

(b) Vertical (left column) and horizontal (right column) accelerations under the 4 Configurations - Optimized joint trajectories.

Fig. 3: Acceleration measurement [g] of 4 boom configurations ($g = 9.81$ m/s^2).

C. Discussion

The experiments validate the vibration reductions of the optimized trajectories that use the proposed approach for all 4 boom configurations, i.e., around 28% in Table II. This is lower than the performance in simulations, e.g., 67.5% in Table I. This discrepancy between the simulation and the reality might be explained by the limitation of trajectory implementation and the fidelity of our simulation model. For example, the sampling frequency of the trajectory input, the nonlinear dynamics, and the actuation frequency of the manipulator joint can contribute to the difference in practical implementation, while a simulation model usually assumes an ideal sampling rate and linear actuation. However, this instead demonstrates the effectiveness of the dynamics-based

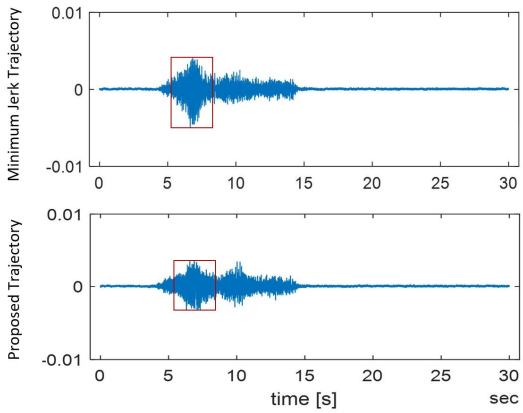

Fig. 4: Comparison: *Minimum jerk trajectory* (top) vs *Proposed optimized trajectory* (bottom) of Configuration 4 horizontal acceleration measurement [g] (g $= 9.81$ m/s^2).

optimization under the uncertainty of a simulation model.

Our procedure for generating the high-order polynomial trajectory can guarantee the zero-boundary condition for a *flexible* number of optimization parameters and a *flexible* number of waypoints. This is radically different from the standard minimum acceleration/jerk trajectories [12]–[14]. Fig. 4 shows a supplementary experimental result of such comparison where the proposed dynamics-based optimized trajectory reduces vibration further. The minimum jerk trajectory is derived via the Euler-Lagrangian method where the order of the polynomial, i.e., the number of parameters, is fixed[2]. A fixed number of parameters is often limited for multi-objective optimization (as it optimizes jerk only), and it becomes inefficient when waypoints are needed. Waypoints are commonly dealt with by connecting a set of minimum jerk trajectories that have the same-order of polynomial at their boundaries, while forcing the time derivatives at the boundaries to zero. This can be problematic in the case of minimizing non-zero derivatives at the waypoints, whilst the proposed method is not bound by such limitation.

V. CONCLUSION

The proposed dynamics-based trajectory planning approach has led to effective vibration reduction. By following the dynamics modeling and trajectory generation procedure, the methodology should be easily transferable to a wider range of flexible long-reach robotic manipulator systems with similar characteristics, e.g., the long-reach system at Fukushima Daiichi. Similar tasks will also be carried out in nuclear fusion engineering of the Joint European Torus (JET) either by a more specialized TWD or the rather versatile MASCOT system in a structure equivalent to the TWD system. The development of advanced knowledge on the specialized TWD system will underpin the understanding of the deployment of any new control strategies in the remote maintenance or decommissioning system at JET. Future work will incorporate the trajectory planning approach with active H_∞ feedback control of the manipulator for external disturbance rejection.

[2]Using the Euler-Lagrangian method, the necessary condition of a minimum acceleration trajectory is a third-order polynomial $x(t) = c_0 + c_1 t + c_2 t^2 + c_3 t^3$ and the necessary condition of a minimum jerk trajectory is a fifth order polynomial $x(t) = c_0 + c_1 t + c_2 t^2 + c_3 t^3 + c_4 t^4 + c_5 t^5$ with t being time and $c_0, \ldots c_5$ being design parameters.

ACKNOWLEDGMENTS

The work was funded by the UK Atomic Energy Authority (UKAEA) within the scope of the LongOps program. The work was partially funded by the Advanced Machinery Productivity Institute (AMPI), and supported by UKAEA/EPSRC Fusion Grant 2022/27 (EP/W006839/1) for fusion decommissioning. The views expressed in this paper are those of the authors and not necessarily those of the Authority. The authors would like to express their gratitude to Sellafield for their generous support throughout the LongOps project. Thanks also to Dr. Keir Groves for his valuable advice about the vibration testing.

REFERENCES

[1] Z. Du, G. Ouyang, J. Xue, and Y. Yao, "A review on kinematic, workspace, trajectory planning and path planning of hyper-redundant manipulators," in *2020 10th Institute of Electrical and Electronics Engineers International Conference on Cyber Technology in Automation, Control, and Intelligent Systems (CYBER)*. IEEE, 2020, pp. 444–449.

[2] A. Gasparetto, P. Boscariol, A. Lanzutti, and R. Vidoni, "Path planning and trajectory planning algorithms: A general overview," *Motion and Operation Planning of Robotic Systems: Background and Practical Approaches*, pp. 3–27, 2015.

[3] A. A. Ata, "Optimal trajectory planning of manipulators: a review," *Journal of Engineering Science and technology*, vol. 2, no. 1, pp. 32–54, 2007.

[4] A. Takata and G. Endo, "Dynamics-based control and path planning method for long-reach coupled tendon-driven manipulator," *Journal of Robotics and Mechatronics*, vol. 36, no. 1, pp. 30–38, 2024.

[5] Y. Li, S. S. Ge, Q. Wei, T. Gan, and X. Tao, "An online trajectory planning method of a flexible-link manipulator aiming at vibration suppression," *IEEE Access*, vol. 8, pp. 130 616–130 632, 2020.

[6] Z. Qiu, C. Li, and X. Zhang, "Experimental study on active vibration control for a kind of two-link flexible manipulator," *Mechanical Systems and Signal Processing*, vol. 118, pp. 623–644, 2019.

[7] Z. Mohamed, J. Martins, M. Tokhi, J. S. Da Costa, and M. Botto, "Vibration control of a very flexible manipulator system," *Control Engineering Practice*, vol. 13, no. 3, pp. 267–277, 2005.

[8] Z. Mohamed and M. O. Tokhi, "Command shaping techniques for vibration control of a flexible robot manipulator," *Mechatronics*, vol. 14, no. 1, pp. 69–90, 2004.

[9] Z. Mohamed, A. Chee, A. M. Hashim, M. O. Tokhi, S. H. Amin, and R. Mamat, "Techniques for vibration control of a flexible robot manipulator," *Robotica*, vol. 24, no. 4, pp. 499–511, 2006.

[10] A. Abe, "Trajectory planning for residual vibration suppression of a two-link rigid-flexible manipulator considering large deformation," *Mechanism and Machine Theory*, vol. 44, no. 9, pp. 1627–1639, 2009.

[11] L. Cui, H. Wang, and W. Chen, "Trajectory planning of a spatial flexible manipulator for vibration suppression," *Robotics and Autonomous Systems*, vol. 123, p. 103316, 2020.

[12] MathWorks, "Minimum jerk polynomial trajectory," https://uk.mathworks.com/help/uav/ref/minimumjerkpolynomialtrajectory.html, accessed: 2024-07-30.

[13] A. Bry, C. Richter, A. Bachrach, and N. Roy, "Aggressive flight of fixed-wing and quadrotor aircraft in dense indoor environments," *The International Journal of Robotics Research*, vol. 34, no. 7, pp. 969–1002, 2015.

[14] C. Richter, A. Bry, and N. Roy, "Polynomial trajectory planning for aggressive quadrotor flight in dense indoor environments," in *Robotics Research: The 16th International Symposium ISRR*. Springer, 2016, pp. 649–666.